Talanta 125 (2014) 114–124

Contents lists available at ScienceDirect

Talanta

journal homepage: www.elsevier.com/locate/talanta

A new spectral deconvolution – Selected ion monitoring method for the analysis of alkylated polycyclic aromatic hydrocarbons in complex mixtures

Albert Robbat Jr.*, Nicholas M. Wilton

Tufts University, Department of Chemistry, 62 Talbot Avenue, Medford, MA 02155, USA

ARTICLE INFO

Article history:
Received 27 January 2014
Received in revised form
25 February 2014
Accepted 26 February 2014
Available online 5 March 2014

Keywords:
Alkylated PAH
Gas chromatography/mass spectrometry
Selected-ion monitoring
Multiple fragmentation patterns per homolog
Detection limits
Narcosis

ABSTRACT

A new gas chromatography/mass spectrometry (GC/MS) method is proffered for the analysis of polycyclic aromatic hydrocarbons (PAH) and their alkylated homologs in complex samples. Recent work elucidated the fragmentation pathways of alkylated PAH, concluding that multiple fragmentation patterns per homolog (MFPPH) are needed to correctly identify all isomers. Programming the MS in selected ion monitoring (SIM) mode to detect homolog-specific MFPPH ions delivers the selectivity and sensitivity that the conventional SIM and/or full scan mass spectrometry methods fail to provide. New spectral deconvolution software eliminates the practice of assigning alkylated homolog peaks via pattern recognition within laboratory-defined retention windows. Findings show that differences in concentration by SIM/molecular ion detection of C_1–C_4 PAH, now the standard, yield concentration differences compared to SIM/MFPPH of thousands of percent for some homologs. The SIM/MFPPH methodology is also amenable to the analysis of polycyclic aromatic sulfur heterocycles (PASH) and their alkylated homologs, since many PASH have the same *m/z* ions as those of PAH and, thus, are false positives in SIM/1-ion PAH detection methods.

1. Introduction

Is peak pattern recognition by selection ion monitoring (SIM) of only molecular ion signals selective enough to accurately measure alkylated polycyclic aromatic hydrocarbons (PAH)? The motivation to address this question is two-fold. First, a disagreement occurred as to whether losses in sensitivity due to full scan mass spectrometry compared to SIM detection of the molecular ion (SIM/1-ion) affect risked-based decisions [1]. Second, is it possible to analyze alkylated PAH in complex samples by SIM using the ions from multiple fragmentation patterns per homolog (MFPPH) without sacrificing sensitivity or selectivity? In this context, we reviewed more than 400 papers published over the last 15 years. We found that 70% of the alkylated PAH literature relied on SIM data and, of these, 71% employed SIM/1-ion detection; the remainder used 2 ions to confirm identity. In addition, the methods published by the US EPA [2], ASTM [3] and NOAA [4] rely solely on the analyst's ability to recognize the C_1–C_4 molecular ion peak patterns for these homologs.

These findings are exemplified in a recent interlaboratory study authored by the National Institute for Standards and Technology (NIST) [5]. A total of 33 laboratories analyzed parent and alkylated PAH in marine sediment. Results showed that the average relative standard deviation (RSD) for the mean parent PAH concentrations was 37%. In contrast, the average %RSD for the homologs studied was 53%, which was biased high by the more alkylated homologs. Since NIST asked each laboratory to use its own proprietary method, the study was unable to conclude why differences in alkylated PAH concentrations were higher than those of parent compounds.

To address these questions, we elucidated the electron impact fragmentation mechanisms of alkylated PAH and their sulfur analogs (the polycyclic aromatic sulfur heterocycles, PASH) by exhaustively analyzing fresh and weathered coal tar and crude oil samples [6,7]. Automated sequential, 2-dimensional gas chromatography (GC–GC) was used to separate matrix components from target compounds. When coelution occurred, simultaneous MS and pulsed flame photometric, sulfur-specific detection differentiated alkylated PAH from PASH. From this work, homolog retention windows and more than 70 unique C_1–C_4 spectral patterns were obtained. Substituent locations on the aromatic ring produced substantive differences in their electron impact fragmentation patterns. We also studied the retention behavior of 119 two- to six-ring parent and alkylated PASH and deduced their fragmentation mechanisms [8]. In addition, we include the results of two National Environmental Laboratory Accreditation Conference (NELAC) laboratories, whose standard operating procedures we have.

* Corresponding author. Tel.: +1 617 627 3474.
E-mail address: albert.robbat@tufts.edu (A. Robbat Jr.).

http://dx.doi.org/10.1016/j.talanta.2014.02.068
0039-9140

Based on these findings, a new SIM/MFPPH method is proposed that provides the selectivity and sensitivity expected of high quality data used to support environmental forensics, toxicity studies, and hazardous waste site investigation and clean-up projects. Although the experimental protocol focuses on PAH in contaminated soil and sediment, the method provides the basis to analyze parent and alkylated PAH and PASH in any complex matrix. Unlike the EPA, ASTM and NOAA methods, which state that experienced analysts are needed to obtain high quality data, presumably to recognize homolog peak patterns, the SIM/MFPPH method uses new, automated spectral deconvolution software that quickly compares the quality of fit between sample and library spectra. The deconvolution software subtracts additive ion current from target ion signals due to matrix ions when it occurs. Examples will illustrate why SIM/1-ion detection methods fail to provide accurate alkylated homolog measurements.

2. Experimental

2.1. Materials

Standards were purchased from Restek (Bellefonte, PA), viz., instrument calibration (16 PAH), internal standard (1,4-dichlorobenzene-d4, naphthalene-d8, phenanthrene-d10, chrysene-d12, and perylene-d12), and surrogate (2-methylnaphthalene-d10 and fluoranthene-d10) mixtures. Dichloromethane and toluene were obtained from Sigma-Aldrich (St. Louis, MO). Hydromatrix was purchased from Agilent Technologies, Inc. (Santa Clara, CA) and high-purity helium gas from Airgas (Salem, NH).

2.2. Sample preparation/extraction

A coal tar impacted soil (sample 1) and two sediment samples (2 and 3) were collected from shuttered manufactured gas plant (MGP) sites in Indiana and New York, respectively. These samples were stored in a freezer at −20 °C until needed. After removal, the samples were warmed to room temperature and then homogenized in 20 g sample batches in 50 mL beakers. From this, 2 g was weighed, dried overnight at 95 °C, and reweighed to determine percent moisture. 5 mg of each sample was analyzed to determine total organic carbon (TOC) using an Elementar analyzer (Hanau, Germany).

Samples were extracted using an automated pressurized liquid extraction and solvent evaporation system from Fluid Management Systems (FMS, Watertown, MA). 10 µL of a 2000 µg/mL surrogate solution was injected into 15 g of sample. Also added were 1 g of copper granules (30 mesh from Restek) and enough Hydromatrix to fill the dead volume in 40 mL extraction cell. The FMS system delivered solvent to the extraction cell, pressurized it, and then transferred the extracts to the evaporator where they were concentrated to 1 mL under gentle heating and nitrogen flow; see Table 1 for programming conditions. The extracts were reconstituted to 5 mL in methylene chloride, and then put into 2 mL vials with 10 µL of the internal standard solution.

Table 1
Sample preparation programming conditions.

Solvent	120 mL 50:50 methylene chloride/toluene
Extractor	Fill chamber with solvent, 2.4 min; pressurize to 1500 psi, 2.5 min; heat to 120 °C, 5 min; maintain at 120 °C and 1500 psi, 20 min; cool to RT, 20 min; depressurize, 0.1 min; rinse with solvent, 1.3 min; N_2 gas purge, 1 min
Evaporator	60 °C, 12 psi N_2 purge

2.3. Gas chromatography/mass spectrometry

The SIM/MFPPH method is designed for routine analysis. A Shimadzu (Baltimore, MD) model QP2010+GC/MS was used; see Table 2 for operating conditions. A test solution consisting of a highly impacted coal tar sediment (~6000 µg/g total PAH) was analyzed by full scan MS to obtain parent and alkylated PAH retention times and to establish the SIM data acquisition windows. Table 3 lists the MS acquisition range for parent PAH and their homologs as a function of retention index and confirming ion abundances normalized to the molecular ion [9,10]. Calculation of the retention index windows is based on using naphthalene, phenanthrene, chrysene, and benzo(g,h,i)perylene as bracketing compounds:

$$index = 100\left(N + \frac{(t_{r,W} - t_{r,1})}{(t_{r,2} - t_{r,1})}\right)$$

where N is the number of aromatic rings in the first bracketing compound, $t_{r,1}$ and $t_{r,2}$ are, respectively, the retention times for the first and second bracketing compounds and $t_{r,W}$ is either the start or stop time for the data acquisition window or the analyte retention time. The data acquisition window start and stop times were set ~20 s before the first compound and after the last compound in the acquisition window eluted. For some alkylated PAH, homolog isomers eluted in more than one data acquisition window. The data analysis software automatically integrates all confirmed isomers independent of where they elute and calculates the total peak area for that homolog.

GC/MS-PFPD was used during method development to confirm sulfur identity when PASH and PAH eluted within the same retention window. Instrument specifics and PASH fragmentation patterns have been published [6–8].

2.4. Initial and continuing calibration

Before each study, an initial calibration curve was established spanning the linear range of the instrument, i.e., from 20 µg/mL to 10 ng/mL for most compounds. Response factors (RF) were calculated at each concentration as follows:

$$RF_i = \frac{(area_i \times conc_{IS})}{(area_{IS} \times conc_i)}$$

where subscripts i and IS for concentration and area correspond to a specific PAH and internal standard, respectively. The instrument was considered in control when the relative standard deviation (RSD) of the initial calibration average RF, $\overline{RF}$, was ≤20% and the correlation coefficient, r^2, was ≥0.99. Continuing calibration measurements were performed at the beginning, middle, and end of each day using the midpoint calibration concentration. The instrument was in control when the initial and continuing calibration relative percent difference (RPD) was ≤20%. Since calibration standards for all alkylated PAH are

Table 2
GC/MS operating conditions.

Column	Rxi-5MS (30 m × 0.25 mm × 0.25 µm)
Temperature program	60 °C for 1 min, 6.5 °C/min to 320 °C, hold for 5 min
Injection volume (µl)	1
Inlet temperature (°C)	320
Head pressure (kPa)	100
Carrier gas	Helium
Purge time (min)	1
Interface temperature (°C)	280
Ion source temp (°C)	230
Ion voltage (eV)	70
Full-scan	50–350 m/z, 240 msec/scan
SIM dwell time	8 msec/ion

Table 3
MS acquisition range, PAH, their ions and relative abundances.

MS acquisition window (start to stop index range)	PAH	Target ions and relative abundances (%)
solvent delay - 262.7 3.0 min – 16.6 min[b]	Naphthalene-d8 (IS)[a]	136(100), 108(12), 137(10)
	Naphthalene	128(100), 129(11), 127(11)
	C_1 Naphthalene	**A**: 142(100), 141(80), 115(30), 143(12)
	C_2 Naphthalene	**A**: 156(100), 141(182), 155(33), 115(22); **B**: 156(100), 141(85), 155(30), 115(15); **C**: 141(100), 156(98), 155(30), 115 (23), 128(16); **D**: 156(100), 141(75), 155(18), 157(13), 115(13); **E**: 156(100), 141(55), 155(30), 115(12)
	C_3 Naphthalene	**A**: 170(100), 141(385), 115(69), 142(46); **B**: 170(100), 155(333), 153(60), 128(57), 156(47); **A**: 170(100), 155(154), 77(31), 153(29), 115(22); **D**: 170(100), 155(182), 153(51), 128(36), 156(24); **E**: 170(100), 155(91), 153(21), 169(18), 171(14); **F**: 170(100), 155(133), 153(40), 128(27), 152(25); **G**: 170(100), 141(333), 115(233), 142(40); **H**: 170(100), 155(75), 169(17), 153(16), 171(14); **I**: 170(100), 155(58), 169(17), 171(14), 153(11); **J**: 170(100), 155(250), 128(155), 115(80), 127(68); K: 170(100), 155(109), 153(23), 152(20), 169(21)
	2-methylnaphthalene-d10 (S)[a]	152(100), 150(81), 151(18)
	Acenaphthylene	152(100), 153(15), 151(14)
	Acenaphthene-d10 (IS)	162(100), 164(96), 160(46)
	Acenaphthene	153(100), 154(83), 152(51)
262.7 - 295.8 16.6 min - 20.5 min	C_3 Naphthalene[c]	See target ion above
	C_4 Naphthalene	**A**: 184(100), 169(200), 154(40), 170(30); **B**: 184(100), 169(68), 185(15), 153(12); **C**: 184(100), 169(125), 185(15), 153(12); **D**: 184(100), 169(92), 153(21), 141(15); **E**: 184(100), 169(105), 153(26), 165(26), 170(16); **F**: 184(100), 155(333), 156(47), 153(40); **G**: 184(100), 141(250), 142(125), 115(63); **H**: 184(100), 141(333), 142(240), 115(77); **I**: 184(100), 141(333), 142(67), 115(33); **J**: 184(100), 169(333), 141(153), 129(153), 128(57); **K**: 184(100), 169(333), 141(100), 129(50), 128(50)
	Fluorene	166(100), 165(84), 167(14)
	C_1 Fluorene	**A**: 180(100), 165(133), 178(33), 179(33); **B**: 180(100), 165(106), 178(27), 179(27), 166(16); **C**: 180(100), 165(93), 179(22), 178(20), 181(15)
295.8 - 339.6 20.5 min – 25.0 min	C_1 Fluorene	See target ions above
	C_2 Fluorene	**A**: 194(100), 179(91), 89(17), 180(16); **B**: 194(100), 179(125), 89(25), 180(21); **C**: 194(100), 179(153), 178(78), 89 (39), 180(32); **D**: 194(100), 165(400), 166(140), 180(10); **E**: 194(100), 179(250), 180(35), 89(25); **F**: 194(100), 165 (263), 166(42)
	C_3 Fluorene	**A**: 208(100), 165(263), 166(105), 164(26); **B**: 208(100), 165(200), 179(160), 178(96), 166(40); **C**: 208(100), 193 (181), 178(87), 194(45)
	Phenanthrene-d10 (IS)	188(100), 189(14), 80(14)
	Phenanthrene	178(100), 176(20), 179(15)
	Anthracene	178(100), 179(16), 176(14)
	C_1 Phenanthrene	**A**: 192(100), 191(55), 189(30), 193(17), 190(15); **B**: 192(100), 191(39), 189(20), 193(15), 190(10)
	C_2 Phenanthrene	**A**: 206(100), 191(142), 189(29), 192(29); **B**: 206(100), 191(85), 189(16), 89(15); **C**: 206(100), 191(35), 189(29), 205 (25); **D**: 206(100), 191(51), 189(27), 205(20); **E**: 206(100), 191(20), 205(20), 189(17); **F**: 206(100), 191(40), 189 (18), 205(16)
339.6 - 356.4 25.0 min – 26.7 min	C_3 Fluorene	See target ions above
	C_2 Phenanthrene	See target ions above
	C_3 Phenanthrene	**A**: 220(100), 205(118), 189(53), 206(35); **B**: 220(100), 205(58), 189(21), 221(18), 101(18); **C**: 220(100), 205(167), 206(35), 189(33); **D**: 220(100), 205(77), 221(30), 189(21), 101(18); **E**: 220(100), 205(41), 221(18), 189(16), 101 (10); **F**: 220(100), 205(52), 221(27), 101(13)
	Fluoranthene-d10 (S)	212(100), 213(19), 210(14)
	Fluoranthene	202(100), 203(17), 200(15)
	Pyrene	202(100), 203(17), 200(15)
356.4 - 390.1 26.7 min – 30.1 min	C_3 Phenanthrene	See target ions above
	C_4 Phenanthrene	**A**: 234(100), 219(75), 204(31), 203(23), 235(20); **B**: 234(100), 219(60), 235(21), 204(17), 189(13); **C**: 234(100), 191(243), 192(129), 189(63), 165(54)
	C_1 Pyrene	**A**: 216(100), 215(71), 217(17), 213(16); **B**: 216(100), 215(37), 217(18), 108(13), 213(12)
	C_2 Pyrene	**A**: 230(100), 113(68), 101(26); **B**: 230(100), 229(35), 215(29), 231(19), 228(14); **C**: 230(100), 231(21), 101(13), 113 (12)
390.1 - 436.8 30.1 min – 34.3 min	C_2 Pyrene	See target ions above
	C_3 Pyrene	**A**: 244(100), 113(55), 229(45), 101(23), 149(21); **B**: 244(100), 229(65), 228(19), 230(15)
	Benz[a]anthracene	228(100), 226(28), 229(20)
	Chrysene-d12 (IS)	240(100), 236(25), 241(17)
	Chrysene	228(100), 226(27), 229(20)
	C_1 Chrysene	**A**: 242(100), 241(23), 243(20), 121(11); **B**: 242(100), 241(57), 239(42), 120(19), 243(19); **C**: 242(100), 241(35), 239(32), 243(20), 240(12); **D**: 242(100), 241(48), 243(30), 226(15)
	C_2 Chrysene	**A**: 256(100), 241(76), 239(53), 240(25), 257(23); **B**: 256(100), 239(53), 240(25), 257(23), 241(22)
436.8 to end of run 34.3 min to 46.0 min	C_1 Chrysene	See target ions above
	C_2 Chrysene	See target ions above
	C_3 Chrysene	**A**: 270(100), 239(33), 271(35), 255(23)
	C_4 Chrysene	**A**: 284(100), 269(128), 270(64)
	Benzo[b]fluoranthene	252(100), 253(22), 250(18)
	Benzo[k]fluoranthene	252(100), 253(21), 250(21)
	Benzo[e]pyrene	252(100), 250(22), 253(22)
	Benzo[a]pyrene	252(100), 253(22), 250(17)
	Perylene-d12 (IS)	264(100), 260(24), 265(22)
	Perylene	252(100), 253(22), 250(22)
	Indeno[1,2,3-cd]pyrene	276(100), 277(23), 274(20)
	Dibenz[a,h]anthracene	278(100), 279(24), 276(17)
	Benzo[ghi]perylene	276(100), 277(24), 138(24)

Notes:

[a] (IS)=internal standard, (S)=surrogate.

[b] Ion group start/stop times correspond to GC/MS temperature programming employed in this study, see Table 2.

[c] Some homologs appear in multiple acquisition windows.

not available, the parent $\overline{RF}$ was used to determine homolog concentrations. It is understood that RF for parent and alkylated PAH are not the same [11,12]; thus, the lack of calibration standards is a limitation of this method and of environmental forensic studies in general. Since the fragmentation pattern for benzo(a)pyrene is essentially the same as those of perylene and benzo(e)pyrene, its $\overline{RF}$ was used to measure the concentration of these compounds.

2.5. Data analysis

The Ion Analytics (Andover, MA) spectral deconvolution software was used to quantify PAH. Parent and alkylated PAH concentrations were calculated in the sample extract as follows:

$$conc_{i,ext} = \frac{(area_i \times conc_{IS})}{(area_{IS} \times \overline{RF})}$$

where $conc_{i,ext}$ is the concentration of a given PAH in the extract; all other terms are defined above. The concentration in the sediment, $conc_{i,sed}$, is expressed on a dry weight basis and is calculated as

$$conc_{i,sed} = \frac{conc_{i,ext} \times vol_{ext}}{wt_{sed}}$$

where vol_{ext} is the total volume of extract and wt_{sed} is the sediment dry weight.

Laboratories A and B (NELAC-certified) were contracted by the site owners to participate in our interlaboratory study. The laboratories determined homolog concentrations by SIM/1-ion (molecular ion) detection based on their respective standard operating procedures. To minimize interlaboratory errors, we reanalyzed the samples using SIM/MFPPH conditions, but processed the data files using each laboratory's homolog-specific retention windows. We also analyzed the data files using the average retention window found in the literature for each homolog. Thus, differences in SIM/MFPPH and SIM/1-ion concentrations are due solely to the retention window differences in each method. Unlike alkylated PAH both laboratories detect 3 ions per parent, which is customary when analyzing samples by full scan mass spectrometry.

2.6. Accuracy and precision

Field and laboratory control check samples were analyzed by SIM/1-ion and SIM/MFPPH to determine accuracy and bias. Method performance was deemed acceptable when concentrations were $\pm 30\%$ of the measured amounts. Measurement precision was determined by analyzing one sample extract in triplicate per day (beginning/middle and middle/end), with an acceptance criterion of $\leq 20\%$ RSD.

2.7. Detection limits

The instrument detection limit (IDL) was determined by analyzing seven identically-prepared standards whose concentration produced a signal-to-noise of 10. The IDL for each parent PAH was calculated as follows: $IDL = SD \times Student's\ t$, where SD is the standard deviation for the seven analyses and $Student's\ t$ corresponds to the one-handed value at 6 degrees of freedom and 99% confidence [13]. From the IDL, the 95% confidence intervals were calculated for each compound's lower and upper limit (LCL and UCL): $LCL = IDL \times 0.64$ and $UCL = IDL \times 2.20$. To compare SIM/1-ion and MFPPH detection limits, the latter method's confirming ions were omitted from MS acquisition, yielding 9 versus 27 ions per detection group.

3. Results and discussion

The most reliable method for identifying compounds in complex mixtures by GC/MS is to compare their molecular and confirming ions against known spectra. In contrast, alkylated PAH are typically identified by their molecular ions and, thus, homolog concentrations by their peak patterns [2–4,12,14,15]. Mis-assignment occurs when PASH and other matrix compounds with common ions elute within the same retention window [6–8,11] or when retention windows are ascribed incorrectly [16]. These error sources typically produce false positives and overestimated concentrations. The MFPPH method detects both the molecular ion and at least two confirming ions for all PAH. The strength of this new method is that it employs spectral deconvolution to identify target compounds as many alkylated PAH fragmentation patterns and ions as needed to correctly quantify homolog concentrations.

3.1. Spectral deconvolution of gas chromatography/mass spectrometry data

Although all data analysis software can extract ion signals, the spectral deconvolution software ensures that only target compounds are quantified and that their signals are differentiated from the matrix. For example, Fig. 1A displays the C_1 phenanthrene elution range and total ion current (TIC) chromatogram for compounds in sample 3, see Table 4 MFPPH retention index windows. When the molecular ion signal m/z 192 (blue) and confirming ions m/z 193 (purple), 191 (green), 190 (maroon), and 189 (cyan) are extracted from the chromatogram, peaks 1, 2, 3, and 6 meet the relative abundance criterion of pattern A in Table 3, see Fig. 1B.

Although peaks 4 and 5 overlap, ion relative abundances for peak 5 match the ion ratios of pattern A after deconvolution. To help visualize the match, the software normalizes confirming ions to the molecular ion at each peak scan after the background signal for each qualifier ion is subtracted from the peak signal (in this case pattern A ions), see Fig. 1C. The reduced ion intensity (relative to the molecular

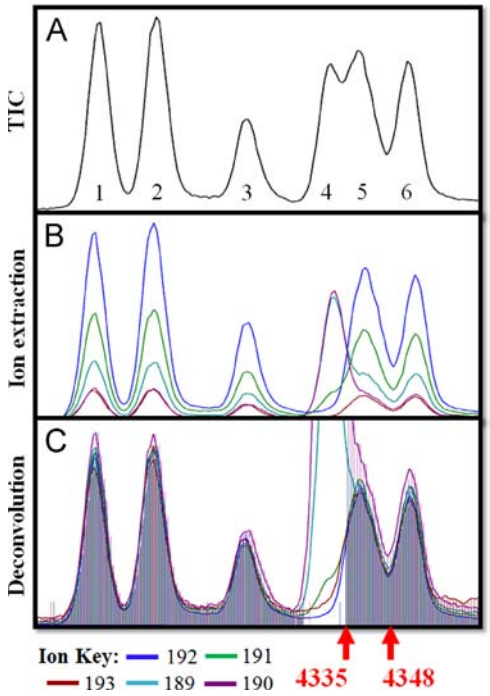

Fig. 1. Sample 3 - spectral deconvolution of C_1 phenanthrene from total ion current chromatogram. (Please see web version for interpretation of color in figure.)
Notes: A) Total ion current (TIC) of C_1 phenanthrene elution range. B) Selected ion extraction of molecular and confirming ions from TIC chromatogram reveals peaks 1, 2, 3, and 6 are C_1 phenanthrene compounds. C) Spectral deconvolution confirms ion extraction results; it also reveals peak 5 as a C_1 phenanthrene and peak 4 as a non-target matrix compound.

ion, $i=1$), $I_i(t)$, at scan (t) is defined as follows:

$$I_i(t) = \frac{A_i(t)}{R_i A_1}$$

where $A_i(t)$ is the intensity of the ith ion and R_i is the expected abundance ratio of that ion to the molecular ion for the target compound. For signals that meet the ion signal ratio criterion (i.e., $\pm 20\%$ for at least four consecutive scans), the molecular and confirming ions appear at the same height. The resulting histogram makes it easy for analysts to confirm peak assignments made by the software and to ensure that only those peaks that belong to the targeted homolog are integrated.

Another compound identity criterion, ΔI, is the spectral match of the average deviation of reduced ion intensities of N confirming ions:

$$\Delta I = \frac{\sum_{i=1}^{N-1}\sum_{j=i+1}^{N}|I_i - I_j|}{\sum_{i=1}^{N-1} i}$$

The closer this value is to zero the more similar all scans are to one another. If signal from a matrix ion adds to a method ion, peaks 4 and 5 in Fig. 1B, the software attempts to eliminate it by computing the relative error (RE) signal at each acceptable scan; then, it subtracts the additive ion signal from the matrix for those scans where interference is observed. An acceptable match is determined by the equation $\Delta I \le K + \Delta_0/A_1$, where the acceptable relative percent difference,K, is set by the analyst and Δ_0 is the additive error from instrument noise or background signal. This criterion measures both the ΔI at each scan and the variance between scans. If the relative intensity of a confirming ion is larger than it should be due to matrix interferences, the algorithm compares all ion ratio relative errors and subtracts the additive ion signal from the matrix ion signal in question. The scan-to-scan variance (ΔE) is calculated from the equation $\Delta E = \Delta I \times \log A_1$. The compound is considered present when ΔI or $\Delta E \le \Delta E_{max}$ in four or more consecutive scans. For this method, the maximum allowable scan-to-scan error,ΔE_{max}, was 7.

Fig. 2 shows the compound details results produced by the software for scans 4327–4354 that correspond to peaks 4–6 in Fig. 1C. When ion ratios meet the acceptance criteria at a given scan, the software lists the molecular ion signal in the compound abundance column if it is designated as the quantitative ion in the method. Also shown are the relative errors at each scan for the C_1 phenanthrene, pattern A ions. If the RE exceeds ΔE_{max}, the compound abundance column is empty, see scans 4327–4334. Since the spectrum for peak 4 fails the identity criteria, the software rejects it as a C_1 phenanthrene compound. Despite contribution of peak

Table 4
Alkylated PAH retention index windows[a].

Compound	MFPPH (Tufts)	Literature	Lab A	Lab B
Naphthalene-d8 (IS)[b]	196.6–202.3	196.6–202.3	196.6–202.3	196.6–202.3
Naphthalene	200	200	200	200
C_1 Naphthalene	218.8–224.7	218.0–225.1	220.3–224.7	220.3–224.7
C_2 Naphthalene	237.3–249.3	231.0–255.5	234.9–249.9	234.8–249.9
C_3 Naphthalene	253.5–273.7	243.4–283.8	252.6–280.9	253.7–274.6
C_4 Naphthalene	274.0–293.2	264.1–303.2	266.4–294.1	266.4–294.4
2–methylnaphthalene-d10 (S)[b]	216.4–222.0	216.4–222.0	216.4–222.0	216.4–222.0
Acenaphthylene	255.8–250.5	255.8–250.5	255.8–250.5	255.8–250.5
Acenaphthalene-d10 (IS)	249.8–255.5	249.8–255.5	249.8–255.5	249.8–255.5
Acenaphthene	250.8–256.5	250.8–256.5	250.8–256.5	250.8–256.5
Fluorene	266.9–272.6	266.9–272.6	266.9–272.6	266.9–272.6
C_1 Fluorene	283.9–297.0	277.2–303.8	273.1–323.9	287.5–292.0
C_2 Fluorene	303.5–314.9	298.5–321.6	289.2–330.1	301.0–316.0
C_3 Fluorene	323.9–334.0	317.9–338.1	293.7–357.1	323.9–343.2
Phenanthrene-d10 (IS)	296.2–302.1	296.2–302.1	296.2–302.1	296.2–302.1
Phenanthrene	300	300	300	300
C_1 Phenanthrene	318.1–325.5	314.6–329.0	304.9–345.0	318.5–325.5
C_2 Phenanthrene	333.1–349.5	327.0–357.7	335.8–350.7	333.1–349.3
C_3 Phenanthrene	351.0–371.1	341.5–381.3	343.2–373.6	343.5–372.1
C_4 Phenanthrene	375.3–380.8	372.8–383.7	388.9–405.5	364.7–388.9
Anthracene	298.4–304.7	298.4–304.7	298.4–304.7	298.4–304.7
Fluoranthene-d10 (S)	340.0–346.6	340.0–346.6	340.0–346.6	340.0–346.6
Fluoranthene	341.5–348.1	341.5–348.1	341.5–348.1	341.5–348.1
Pyrene	349.3–355.9	349.3–355.9	349.3–355.9	349.3–355.9
C_1 Pyrene	362.2–378.9	353.4–387.4	359.7–387.6	359.6–380.5
C_2 Pyrene	378.9–398.2	369.3–410.0	357.2–412.2	None Provided
C_3 Pyrene	394.4–432.0	376.5–448.4	393.9–432.4	None Provided
Benz[a]anthracene	395.3–402.2	395.3–402.2	395.3–402.2	395.3–402.2
Chrysene-d12 (IS)	396.2–402.1	396.2–402.1	396.2–402.1	396.2–402.1
Chrysene	400	400	400	400
C_1 Chrysene	408.7–427.2	399.0–436.2	392.6–432.8	407.4–432.7
C_2 Chrysene	432.3–447.6	424.7–455.0	393.3–455.2	414.9–452.7
C_3 Chrysene	450.3–455.8	447.7–459.0	410.8–482.0	429.2–468.8
C_4 Chrysene	442.7–486.9	420.5–508.9	479.7–501.7	439.7–486.9
Benzo[b]fluoranthene	438.7–446.3	438.7–446.3	438.7–446.3	438.7–446.3
Benzo[k]fluoranthene	439.4–447.1	439.4–447.1	439.4–447.1	439.4–447.1
Benz[e]pyrene	448.5–456.0	448.5–456.0	448.5–456.0	448.5–456.0
Benz[a]pyrene	450.3–457.9	450.3–457.9	450.3–457.9	450.3–457.9
Perylene-d12 (IS)	452.3–459.9	452.3–459.9	452.3–459.9	452.3–459.9
Perylene	453.2–460.8	453.2–460.8	453.2–460.8	453.2–460.8
Indeno[1,2,3–cd]pyrene	488.6–496.2	488.6–496.2	488.6–496.2	488.6–496.2
Dibenz[a,h]anthracene	489.5–497.1	489.5–497.1	489.5–497.1	489.5–497.1
Benzo[ghi]perylene	500	500	500	500

Notes:

[a] Retention index ranges for MFPPH, commercial labs A and B, and literature.

[b] (IS)=internal standard, (S)=surrogate.

4 signal to peak 5, the software eliminates sufficient interference to assign acceptance of scans 4335–4348, i.e., RE→0, see Fig. 2. Only those compounds whose spectrum meets the acceptance criteria at each peak scan are shown as a histogram in Fig. 1C. Note: ion ratios at the rise of peak 5, scans 4331–4334, are badly distorted due to ion signals (*m/z* 189, 190, 191) from the preceding compound. The loss of signal from these few scans is insignificant when compared to the total peak area and has no material effect on concentration.

Finally, two additional criteria must also be met. The first is the *Q*-value, an integer between 1 and 100. It measures the total deviation of the absolute value of the expected minus observed ion ratios divided by the expected ratio multiplied by 100 for each scan in the peak. The closer this number to 100, the greater the certainty between sample and method spectra. The acceptable and calculated *Q*-values for peak 5 were 95 and 98, respectively. The second is the *Q*-ratio, which measures the ratio of the molecular ion peak area to each confirming ion's peak area. This criterion is met when the ion ratios are within ±20% of method values. The peak 5 *Q*-ratios for *m/z* 191, 189, 193 and 190 were 0.58, 0.38, 0.17 and 0.27, respectively,

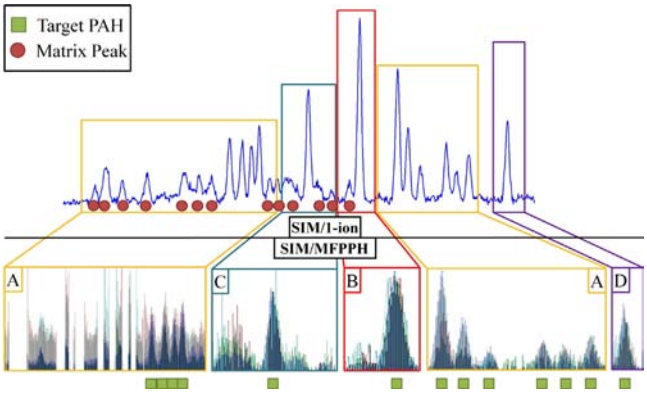

Fig. 3. Sample 2 - C_4 naphthalene SIM/1-ion chromatogram (top) and SIM/MFPPH deconvolved chromatogram (bottom). (Please see web version for interpretation of color in figure.)
Note: Although 26 peaks are discernible in the molecular ion chromatogram of C_4 naphthalene, *m/z* 184, only one-half of the peaks meet MFPPH the compound identity confirmation criterion (green squares).

Details: C1 Phenanthrenes C1PA (2056 scans)

No.	Time [min.]	Rel.Err.	Comp.Ab.	192.0 M/Z (Main)	191.0 M/Z	189.0 M/Z	193.0 M/Z	190.0 M/Z
4327	23.193	83		978	1986	8128	360	8459
4328	23.197	89.6		1109	2314	9812	372	10119
4329	23.202	91		1219	2510	10688	420	11183
4330	23.207	75.9		1526	2562	10719	473	11409
4331	23.211	54.1		2030	2747	10049	594	10512
4332	23.216	34.2		2919	3086	8935	745	9343
4333	23.221	19.2		4270	3497	7606	1029	7646
4334	23.225	10.2		6007	4165	6355	1249	5927
4335	23.230	5.1	8035	8035	4910	5249	1489	4496
4336	23.235	2.7	9952	9952	6015	4595	1816	3626
4337	23.239	1.6	11187	11187	6757	4342	1936	3092
4338	23.244	0.8	12116	12116	7239	3996	2189	2676
4339	23.249	0.7	13197	13197	7864	4239	2172	2671
4340	23.253	0.4	13449	13449	7869	4059	2237	2413
4341	23.258	0.5	12984	12984	7592	4031	2121	2379
4342	23.263	0.4	11509	11509	6753	3664	1919	2084
4343	23.267	0.5	10649	10649	6325	3362	1774	1984
4344	23.272	0.5	9866	9866	5542	3131	1624	1880
4345	23.277	0.6	8152	8152	4714	2664	1374	1611
4346	23.281	0.6	7223	7223	3986	2388	1234	1418
4347	23.286	0.6	6074	6074	3374	2025	1048	1214
4348	23.291	0.7	5182	5182	2964	1839	953	1066
4349	23.295	0.7	4706	4706	2694	1676	849	1004
4350	23.300	0.7	5165	5165	2966	1733	933	1105
4351	23.305	0.7	5963	5963	3541	2064	1034	1236
4352	23.309	0.6	7114	7114	4146	2412	1292	1444
4353	23.314	0.5	9120	9120	5414	2900	1592	1752
4354	23.319	0.5	10711	10711	6295	3524	1817	2006

Show scans All Found 673 in 2056 Print Export

Fig. 2. Sample 3 - C_1 phenanthrene spectral deconvolution software results.
Note: Compound details module shows scan-to-scan RE for peaks 4–6 in Fig. 1. Scans that fail to meet the criterion, RE ≤ 7, are rejected.

and are within the acceptable error of the ion ratios for pattern A. All of the criteria mentioned above form a single compound identity criterion for the SIM/MFPPH method.

3.2. SIM/1-ion versus SIM/MFPPH precision and accuracy

Fig. 3 shows the SIM/1-ion (top) C_4 naphthalene molecular ion, *m/z* 184, chromatogram and the SIM/MFPPH spectral deconvolution chromatogram (bottom) of the homolog's molecular and confirming ions for sample 2. The two NELAC laboratories used the same retention window and included all 26 peaks in their concentration estimate. Only 13 of these meet the identity criterion for fragmentation patterns A–D, see Table 3. Since matrix (red circles) and C_4 naphthalene (green squares) compounds elute within the same integration window, both laboratories reported an elevated concentration, viz., 200 ng/g. In contrast, we found 110 ng/g by SIM/MFPPH. Because matrix components can change from one sample to the next, peak profiles too will change in the chromatogram.

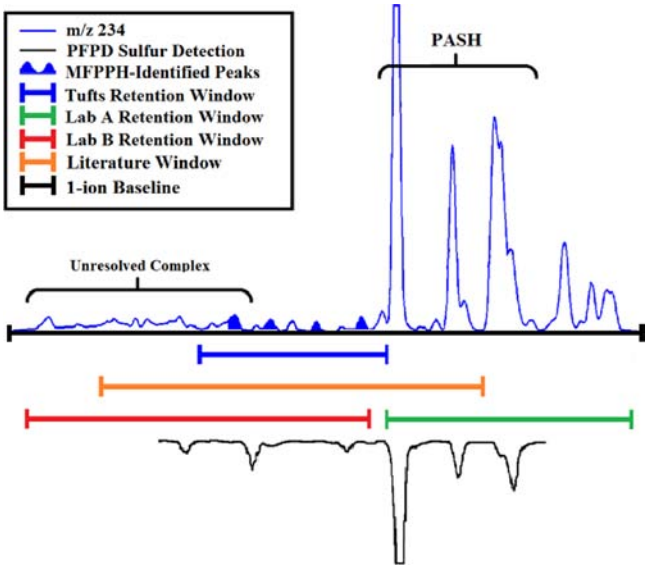

Fig. 4. Sample 1, C_4 phenanthrene molecular ion chromatogram and PFPD chromatogram of same retention range. (Please see web version for interpretation of color in figure.)
Note: C_4 phenanthrene concentrations are retention window dependent if the molecular ion, *m/z* 234, signal area is based solely on peak recognition. PFPD response confirms MFPPH identity of PASH peaks.

Fig. 4 shows the sample 1, C_4 phenanthrene molecular ion chromatogram (top trace) and, below it, the four integration windows used to compare SIM/1-ion and SIM/MFPPH results. The figure depicts the MFPPH (blue bar), literature (orange bar), Laboratory A (green bar), and Laboratory B (red bar) retention windows. A common baseline (black bar) was used to integrate method-specific peaks. Spectral deconvolution of the SIM/MFPPH ions revealed the blue shaded peaks as C_4 phenanthrenes; all three fragmentation patterns meet the identity criterion in Table 3. GC/MS-PFPD (bottom trace) confirmed that peaks identified by MS as alkylated PASH were due to sulfur-containing organics.

Widely different retention windows and the inability to confirm or reject homolog peaks are the main sources of error in SIM/1-ion analyses. Specifically, Laboratory A did not include any of the peaks assigned by MFPPH as C_4 phenanthrenes but did include matrix components (PASH and others) in its concentration estimate. In contrast, Laboratory B included C_4 phenanthrenes, some low level sulfur-containing compounds, and all of the unresolved mixture in its estimate compared to the literature concentration, which included C_4 phenanthrenes, some low and high concentration PASH, and most of the unresolved mixture. All four methods dramatically overestimated the concentration compared to MFPPH, e.g., Laboratory A 2180%, literature 1360%, Laboratory B 371%, and Tufts 176%. Although the same retention window was used for both Tufts methods, SIM/1-ion integrated non-target compound peaks.

Fig. 5 shows the C_1–C_3 fluorene MFPPH integration windows as well as those used by Laboratories A and B for C_1 fluorene. Also depicted in the figure are sample 3 SIM/1-ion peaks for these homologs as well as the C_1 fluorene peaks by spectral deconvolution. Note: the C_1 fluorene molecular ion, *m/z* 180 (blue peaks), is also a minor ion of C_2 and C_3 fluorene. The obvious differences in retention windows, therefore, lead to equally different concentrations. For example, Laboratory B's concentration includes only three of the 11 C_1 fluorene compounds found by MFPPH whereas Laboratory A's concentration is a function of all three homologs. Although these homologs exhibit different molecular ions, Laboratory A included the same peaks (double counting them) in their C_2 and C_3 homolog concentrations.

Table 5 lists the percent misestimation for each homolog as quantified by the SIM/MFPPH and the SIM/1-ion methods. To minimize error sources, the same data files, baselines, and response factors were used to calculate the concentrations. Findings prove that results are retention window dependent, especially if the sole means of identification is pattern recognition. Except for C_1 fluorene and C_1 chrysene, whose sample 2 peaks were near the detection limit,

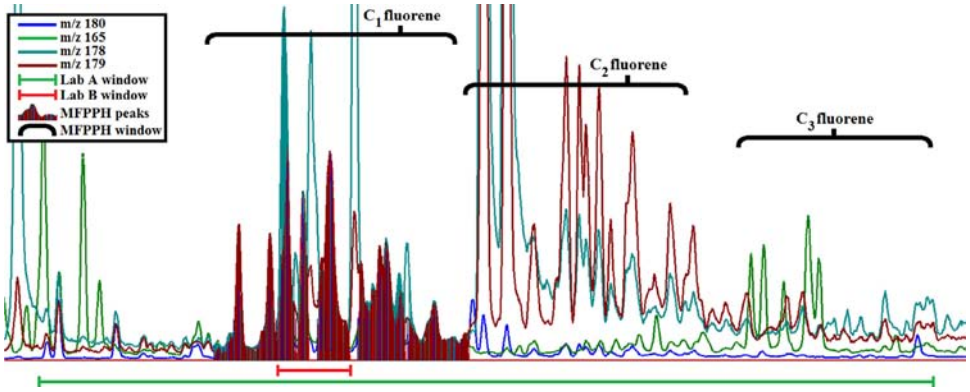

Fig. 5. Sample 3 - matrix compounds that both elute in the C_1 to C_3 fluorene range and yield the same fragment ions as C_1 fluorene. (Please see web version for interpretation of color in figure.)
Note: Spectral deconvolution (pattern A) makes C_1 fluorene peaks obvious. Lab A overestimates the concentration by including matrix compounds (molecular ion, *m/z* 180, blue peaks) in the total homologue peak area count whereas Lab B underestimates the concentration due to false negatives (missed isomers).

all other monoalkylyated homolog concentrations were within the ± 30% accuracy criterion. C_1 homologs have generally narrower retention windows (except for Laboratory A C_1 fluorene) and are higher in concentration relative to their more alkylated homologs. As PAH alkylation increases, failure rates increase with misestimation more likely.

Our results help explain NIST's findings, which show that measuring the true concentration of an alkylated PAH homologue is retention window dependent. Although the mean concentration RSD is 53% for all homologs, many of the laboratories reported concentration differences from one another of hundreds of percent [5]. Accuracy was unpredictable; for example, the mean concentration RSD measured by the 33 participating laboratories was 85% and 40% for C_2 naphthalene and C_3 phenanthrene, respectively.

3.3. SIM/1-ion versus SIM/MFPPH sensitivity

Table 6 lists the %RSD for the average response factor calculated from the standards and correlation coefficients for the calibration curve, which meet method performance requirements of high quality data. To test whether SIM/MFPPH achieves the sensitivity requirements of the most demanding PAH analysis, viz., ASTM D7363, a pore water method, we measured the on-column mass at the IDL. Detection limits for the ASTM method are sub-nanogram/mL [3]. For example, chrysene, the lowest concentration analyte,

Table 5
Percent misestimation[a] in coal tar contaminated samples measured by the SIM/MFPPH and SIM/1-ion methods.

Compounds	Sample 1 (%)				Sample 2 (%)				Sample 3 (%)			
	Tufts	Literature	Lab A	Lab B	Tufts	Literature	Lab A	Lab B	Tufts	Literature	Lab A	Lab B
C1 Naphthalenes	1	2	0	0	0	1	−3	−3	2	2	1	1
C2 Naphthalenes	0	2	0	0	5	24	4	5	3	20	5	7
C3 Naphthalenes	8	12	11	8	9	19	12	9	5	17	11	6
C4 Naphthalenes	79	845	89	89	42	246	82	82	5	76	21	21
C1 Fluorenes	0	38	52	−21	6	35	48	−30	2	21	41	−41
C2 Fluorenes	0	48	121	6	9	41	87	14	6	30	71	8
C3 Fluorenes	288	442	1920	397	0	51	280	49	3	51	239	47
C1 Phenanthrenes	4	8	17	5	4	15	24	4	3	22	28	3
C2 Phenanthrenes	9	20	4	8	7	17	6	8	2	11	2	1
C3 Phenanthrenes	91	158	131	129	46	100	80	75	29	49	45	44
C4 Phenanthrenes	176	1360	2180	371	ND[b]	ND	FP[b]	ND	136	601	571	355
C1 Pyrenes	3	5	5	3	5	9	10	5	4	7	7	4
C2 Pyrenes	29	78	83	n/a[b]	11	33	46	n/a	8	35	42	n/a
C3 Pyrenes	452	542	466	n/a	FP	FP	FP	n/a	FP	FP	FP	n/a
C1 Chrysenes	4	24	18	11	21	54	51	24	6	19	21	8
C2 Chrysenes	1	43	107	90	32	63	105	86	11	81	86	59
C3 Chrysenes	210	363	1270	1130	ND	ND	ND	ND	FP	FP	FP	FP
C4 Chrysenes	441	2090	1340	1470	ND	ND	ND	ND	ND	FP	FP	FP

[a] *Notes*:

$$\%\ Misestimation = 100 * \frac{|conc_{MFPPH} - conc_{1-ion}|}{conc_{MFPPH}}$$

[b] Notes: FP = false positive, ND = homolog was not detected by either the SIM/MFPPH or the comparative method, n/a = retention information was not provided in Lab B's SOP.

Table 6
Response factors and on-column instrument detection limits[a] comparing the full scan, SIM/MFPPH, and SIM/1-ion[b] ($n = 7$).

Compound	SIM/MFPPH					SIM/1-ion					Full Scan				
	R^2	RF (%RSD)	IDL (pg)	LCL	UCL	R^2	RF (%RSD)	IDL (pg)	LCL	UCL	R^2	RF (%RSD)	IDL (pg)	LCL	UCL
Naphthalene	0.9998	1.12 (3)	1.31	0.84	2.87	0.9991	1.21 (9)	0.87	0.56	1.91	0.9980	1.16 (5)	8.03	5.14	17.67
Acenaphthylene	0.9973	1.72 (10)	1.60	1.03	3.53	0.9997	2.24 (5)	0.83	0.53	1.82	0.9993	2.12 (6)	11.71	7.49	25.76
Acenaphthene	0.9969	1.01 (11)	1.55	0.99	3.41	0.9994	1.31 (10)	0.82	0.53	1.81	0.9980	1.32 (5)	8.86	5.67	19.49
Fluorene	0.9965	1.13 (10)	2.09	1.34	4.61	0.9993	1.41 (10)	0.77	0.49	1.68	0.9989	1.39 (2)	40.78	26.10	89.71
Phenanthrene	0.9968	1.09 (5)	1.50	0.96	3.31	0.9988	1.08 (16)	1.03	0.66	2.27	0.9989	1.12 (4)	10.00	6.40	22.00
Anthracene	0.9962	0.92 (13)	1.18	0.76	2.60	0.9990	1.07 (3)	0.86	0.55	1.88	0.9993	1.09 (3)	10.47	6.70	23.04
Fluoranthene	0.9940	1.02 (14)	0.94	0.60	2.07	0.9982	1.28 (8)	0.95	0.61	2.08	0.9994	1.13 (12)	31.55	20.20	69.42
Pyrene	0.9955	1.07 (15)	1.07	0.69	2.36	0.9984	1.30 (9)	0.94	0.60	2.07	0.9991	1.19 (3)	30.69	19.64	67.52
Benz[a]anthracene	0.9973	0.99 (12)	1.41	0.90	3.10	0.9993	1.25 (15)	1.39	0.89	3.06	0.9987	1.12 (8)	34.88	22.33	76.75
Chrysene	0.9966	1.10 (12)	1.26	0.80	2.76	0.9992	1.16 (19)	1.47	0.94	3.24	0.9998	1.19 (6)	16.59	10.62	36.50
Benzo[b]fluoranthene	0.9984	1.25 (13)	1.04	0.66	2.28	0.9996	1.30 (14)	1.42	0.91	3.13	0.9986	1.25 (3)	37.55	24.03	82.60
Benzo[k]fluoranthene	0.9980	1.08 (12)	1.31	0.84	2.89	0.9994	1.39 (4)	1.20	0.77	2.65	0.9987	1.32 (4)	34.77	22.25	76.50
Benzo[a]pyrene	0.9988	0.86 (4)	0.91	0.58	2.00	0.9997	1.24 (4)	1.48	0.95	3.26	0.9974	1.24 (3)	52.42	33.55	115.33
Indeno[1,2,3–cd]pyrene	0.9993	0.60 (18)	1.58	1.01	3.48	0.9998	1.22 (6)	1.42	0.91	3.13	0.9930	1.25 (8)	55.41	35.46	121.89
Dibenz[ah]anthracene	0.9989	0.53 (19)	1.25	0.80	2.75	0.9995	1.18 (7)	1.03	0.66	2.27	0.9926	1.25 (4)	67.48	43.19	148.46
Benzo[ghi]perylene	0.9995	0.81 (10)	2.21	1.41	4.85	0.9998	1.24 (13)	1.23	0.79	2.71	0.9974	1.41 (4)	40.27	25.77	88.59

Notes:

[a] IDL is reported as mass on-column based on 1 uL injection of standards at 10 ng/mL.

[b] Null hypotheses: is SIM/1-ion detection more sensitive than the SIM/MFPPH, while both are more sensitive than full scan ($p < 0.05$).

must be detected at 90 pg in 1.5 mL based on SPME extraction. Assuming 50% SPME efficiency, the performance benchmark for on-column mass detection would be 45 pg. Also shown in the same table are the on-column IDLs for SIM/MFPPH, SIM/1-ion, and full scan MS based on 1 μL injections along with their upper and lower 95% confidence limits. SIM/MFPPH surpasses the benchmark for all PAH. Since the SIM/MFPPH and SIM/1-ion IDLs of ~1.0 pg overlap at the 95% confidence interval, there is no statistical difference between the two methods. As expected, full scan MS produced IDLs 30 times higher than those of SIM.

IDLs were obtained by analyzing standards ($n=7$), whose concentration was 10 ng/mL. The 10:1 *S*/*N* threshold sometimes results in ion skewing from quadrupole instruments. Table 7 lists the extracted ions, relative abundances, and number of peak scans for each PAH in the 10 ng/mL solution. Excellent agreement was obtained between the expected and observed signals as measured by the RE, *Q*-ratio and *Q*-value for each compound at the limit of quantitation.

3.4. Toxic units

To determine if PAH-contaminated soil, sediment, or pore water is toxic to benthic organisms, the U.S. Environmental Protection Agency measures the concentration of 18 parent and 16 PAH homologs using the equilibrium partition model [2,17–19]. The toxic unit (TU) for

Table 7
Expected versus observed deconvolution ion signal ratios at 10 pg on-column.

	# Peak Scans	Ions	Expected RA	Ion Signals	Q-ratio	RE	Q-value
Naphthalene	38	128	100	18,163	–	0.5	98
		129	12	1943	10.7		
		127	13	2090	11.5		
Acenaphthylene	28	152	100	18,601	–	0.1	100
		153	14	2258	12.1		
		151	22	3865	20.8		
Acenaphthene	22	153	100	13,630	–	0.3	97
		154	83	13,112	96.2		
		152	51	7966	58.4		
Fluorene	23	166	100	12,918	–	0.2	98
		165	84	11,930	92.3		
		167	14	1794	13.9		
Phenanthrene	28	178	100	27,033	–	0.2	99
		176	22	5471	20.2		
		179	16	4459	16.5		
Anthracene	26	178	100	25,999	–	0.3	100
		179	16	3873	14.9		
		176	20	4991	19.2		
Fluoranthene	27	202	100	32,141	–	0.1	100
		203	18	5508	17.1		
		200	22	6831	21.3		
Pyrene	22	202	100	32,682	–	0.2	99
		203	17	5455	16.7		
		200	22	7006	21.4		
Benz[a]anthracene	20	228	100	31,680	–	0.1	100
		226	28	8234	26.0		
		229	20	6197	19.6		
Chrysene	28	228	100	34,239	–	0.1	100
		226	32	10,330	30.2		
		229	20	6855	20.0		
Benzo[b]fluoranthene	22	252	100	31,803	–	0.2	99
		253	24	7914	24.9		
		250	28	8372	26.3		
Benzo[k]fluoranthene	28	252	100	32,218	–	0.3	100
		253	23	7283	22.6		
		250	26	8112	25.2		
Benzo[a]pyrene	30	252	100	30,081	–	0.6	99
		253	23	7183	23.9		
		250	28	7698	25.6		
Indeo[123-cd]pyrene	28	276	100	28,534	–	0.3	96
		277	27	8273	29.0		
		274	25	7976	28.0		
Dibenz[ah]anthracene	39	278	100	26,742	–	0.5	95
		279	33	9199	34.3		
		139	28	8087	30.2		
Benzo[ghi]perylene	39	276	100	70,176	–	0.3	98
		277	25	16,437	23.4		
		138	29	17,465	24.9		

Note: Q-ratio acceptance criterion ≤20% of expected RA (relative abundance).

Table 8
Sample 2 PAH concentrations and corresponding toxicity by the SIM/MFPPH and Lab A/B methods.

Parent PAH	Sediment Concentration (mg/kg) All Methods			Toxic Units All Methods		
Naphthalene	0.512			0.0321		
Acenaphthylene	0.536			0.0287		
Acenaphthene	1.060			0.0522		
Fluorene	0.655			0.0294		
Phenanthrene	2.760			0.1120		
Anthracene	1.290			0.0523		
Fluoranthene	1.380			0.0472		
Pyrene	2.700			0.0936		
Benz[a]anthracene	0.927			0.0266		
Chrysene	0.768			0.0220		
Benzo[b]fluoranthene	0.288			0.0071		
Benzo[k]fluoranthene	0.386			0.0095		
Benzo[a]pyrene	0.788			0.0197		
Benzo[e]pyrene	0.421			0.0105		
Perylene	0.120			0.0023		
Indeno[1,2,3–cd]pyrene	0.366			0.0079		
Dibenz[ah]anthracene	0.119			0.0026		
Benzo[ghi]perylene	0.338			0.0075		
Alkylated PAH	**SIM/MFPPH (%RSD)**	**Lab A**	**Lab B**	**SIM/MFPPH**	**Lab A**	**Lab B**
C1 Naphthalene	0.944 ± 9.7	0.920	0.920	0.0513	0.0500	0.0500
C2 Naphthalene	1.360 ± 2.7	1.410	1.420	0.0643	0.0667	0.0673
C3 Naphthalene	0.696 ± 6.1	0.782	0.762	0.0289	0.0325	0.0317
C4 Naphthalene	0.110 ± 3.8	0.200	0.200	0.0040	0.0074	0.0736
C1 Fluorene	1.000 ± 1.4	1.490	0.701	0.0397	0.0588	0.0277
C2 Fluorene	0.407 ± 2.8	0.762	0.470	0.0143	0.0268	0.0164
C3 Fluorene	0.197 ± 7.6	0.748	0.294	0.0062	0.0235	0.0092
C1 Phenanthrene	2.200 ± 3.3	2.740	2.290	0.0794	0.9880	0.0826
C2 Phenanthrene	0.896 ± 6.3	0.948	0.965	0.0290	0.0307	0.0312
C3 Phenanthrene	0.244 ± 2.1	0.439	0.428	0.0071	0.0128	0.0125
C4 Phenanthrene	ND	0.380	ND	ND	0.0100	ND
C1 Pyrene	2.250 ± 3.5	2.470	2.360	0.0706	0.0774	0.0741
C1 Chrysene	0.693 ± 3.2	1.050	0.857	0.0180	0.0273	0.0223
C2 Chrysene	0.193 ± 3.9	0.395	0.358	0.0046	0.0095	0.0086
C3 Chrysene	ND	ND	ND	ND	ND	ND
C4 Chrysene	ND	ND	ND	ND	ND	ND
			TOTAL	0.981	1.09	1.00
			% Diff	–	11	2

each PAH is added and if the total is ≥ 1, the sample is deemed toxic. Overestimated concentrations have a material effect on toxicity. Table 8 lists the concentrations and toxic units for sample 2 when measured by Laboratories A and B and by SIM/MFPPH. This example is illustrative of the impact SIM/1-ion overestimation has on raising the TU when it is just below one. Since parent PAH concentrations are the same, differences in TU are due to the homologs. Also shown in the table is the precision obtained by SIM/MFPPH, which was excellent for each homolog. All RSDs were less than 10% ($n=3$), with most about 3%.

Although Laboratories A and B overestimated the concentration of some homologs by more than 30%, the effect on toxicity is less dramatic. For example, total TU was overestimated by 11% and 2%, respectively, for Laboratories A and B. Nonetheless, laboratory SIM/1-ion inaccuracy elevated the TU above the threshold for toxicity. It should be reemphasized that although the same concentrations for parent PAH were found, inaccuracies in this measurement also contribute to total sample toxicity. In contrast, petrogenic samples contain much more alkylated PAH, as high as 99% compared to parent compounds and, thus, overestimated concentrations would influence the toxicity of oil impacted samples even more than that of coal tar [12].

4. Conclusions

A new GC/MS method is proffered, based on SIM detection of MFPPH ions, for parent and alkylated PAH in complex mixtures. The

method combines the selectivity of full scan mass spectrometry with the sensitivity of SIM analysis, with excellent precision and accuracy by employing new spectral deconvolution software to eliminate the need for analysts to recognize homolog peak patterns or produce false positives/negatives due to incorrect retention windows. Moreover, our findings explain why laboratory-to-laboratory variability is so poor (NIST interlaboratory study), even when sample preparation and data analysis procedures are controlled (our interlaboratory study). Results indicate that differences in homolog retention windows and the analyst's ability to correctly recognize target compounds are the major sources of error.

Acknowledgments

The authors appreciate Shimadzu, USA, Fluid Management Systems, and Gerstel GmbH for instrument contributions used in this work. We recognize the efforts of Yuriy Gankin and Eugene Baydakov for writing the deconvolution software code and Christian Zeigler for the MFPPH ions.

References

[1] S.B. Hawthorne, D.J. Miller, Environ. Sci. Technol. 46 (2012) 11475–11476.
[2] U.S. EPA. Method 8272, Parent and Alkyl Polycyclic Aromatics in Sediment Pore Water by Solid-Phase Microextraction and Gas Chromatography/Mass Spectrometry in Selected Ion Monitoring Mode, Government Printing Office, Washington, D.C., 2007.
[3] ASTM D7363-11, Determination of Parent and Alkyl Polycyclic Aromatics in Sediment Pore Water Using Solid-Phase Microextraction and Gas Chromatography/Mass Spectrometry in Selected Ion Monitoring Mode, ASTM International, West Conshohocken, PA, 2012.
[4] NOAA, Technical Memorandum, NOS ORCA 130. Sampling and Analytical Methods of the National Status and Trends Program, Silver Spring, MD, 1998.
[5] NIST. NISTIR 7792, Interlaboratory Analytical Comparison Study to Support Deepwater Horizon Natural Resource Damage Assessment: Description and Results for Marine Sediment QA10SED0, Government Printing Office, Washington, D.C., 2011.
[6] C.D. Zeigler, A. Robbat Jr, Environ. Sci. Technol 46 (2012) 3935–3942.
[7] C.D. Zeigler, N. Wilton, A. Robbat Jr, Anal. Chem. 84 (2012) 2245–2252.
[8] C.D. Zeigler, M. Schantz, S. Wise, A. Robbat Jr, Polycycl. Aromat. Compd. 32 (2012) 154–176.
[9] W.P. Eckel, T. Kind, Anal. Chim. Acta 494 (2003) 235–244.
[10] K. Héberger, B. Škrbić, Anal. Chim. Acta 716 (2012) 92–100.
[11] C.D. Zeigler, K. MacNamara, Z. Wang, A. Robbat Jr, J. Chromatogr. A 1205 (2008) 109–116.
[12] S.B. Hawthorne, D.J. Miller, J.P. Kreitinger, Environ. Toxicol. Chem. 25 (2006) 287–296.
[13] U.S. EPA. 51 FR 23703, Definition and Procedure for the Determination of the Method Detection Limit, Government Printing Office, Washington, D.C., 1986.
[14] Z. Wang, C. Yang, Z. Yang, J. Sun, B. Hollebone, C. Brown, M. Landriault, J. Environ. Monit. 13 (2011) 3004–3017.
[15] P.S. Daling, L. Fakness, Environ. Forensics 3 (2002) 263–278.
[16] P.M. Antle, C.D. Zeigler, N.M. Wilton, A. Robbat Jr, Intern. J. Environ. Anal. Chem. (2013), http://dx.doi.org/10.1080/03067319.2013.840886.
[17] U.S. EPA. EPA-600-R-02-013, Procedures for the Derivation of Equilibrium Partitioning Sediment Benchmarks (ESBs) for the Protection of Benthic Organisms: PAH Mixtures, Government Printing Office, Washington, D.C., 2003.
[18] D.M. Di Toro, J.A. McGrath, D.J. Hansen, Environ. Toxicol. Chem. 19 (2000) 1951–1970.
[19] D.M. Di Toro, J.A. McGrath, Environ. Toxicol. Chem. 19 (2000) 1971–1982.